

Solid-State Water Electrolysis with an Alkaline Membrane

Yongjun Leng,^{†,‡} Guang Chen,[§] Alfonso J. Mendoza,[§] Timothy B. Tighe,[§] Michael A. Hickner,^{*,§} and Chao-Yang Wang^{*,†,§,||}

[†]Electrochemical Engine Center, [‡]Department of Mechanical and Nuclear Engineering and [§]Department of Materials Science and Engineering, The Pennsylvania State University, University Park, Pennsylvania 16802, United States

^{||}Center for Energy Storage and Conversion, and Department of Energy and Resources Engineering, Peking University, Beijing 100871, China

S Supporting Information

ABSTRACT: We report high-performance, durable alkaline membrane water electrolysis in a solid-state cell. An anion exchange membrane (AEM) and catalyst layer ionomer for hydroxide ion conduction were used without the addition of liquid electrolyte. At 50 °C, an AEM electrolysis cell using iridium oxide as the anode catalyst and Pt black as the cathode catalyst exhibited a current density of 399 mA/cm² at 1.80 V. We found that the durability of the AEM-based electrolysis cell could be improved by incorporating a highly durable ionomer in the catalyst layer and optimizing the water feed configuration. We demonstrated an AEM-based electrolysis cell with a lifetime of >535 h. These first-time results of water electrolysis in a solid-state membrane cell are promising for low-cost, scalable hydrogen production.

Hydrogen is an excellent energy storage medium for renewable and sustainable energy systems.^{1–3} The advantages of hydrogen as an energy carrier include (1) highly efficient reversible conversion between hydrogen and electricity, (2) good energy density of compressed hydrogen storage compared to the energy density of most types of batteries, and (3) scalability of hydrogen technologies for grid-scale applications. Advanced water electrolysis is one of the most efficient and reliable approaches to produce hydrogen from renewable energy such as solar, wind, and hydropower for grid-scale energy storage.^{4–6} There are two main types of low-temperature water electrolysis currently available: alkaline liquid electrolyte water electrolysis,^{7–9} and proton exchange membrane (PEM) water electrolysis.^{10–19}

In alkaline liquid electrolyte water electrolysis, non-precious metals can be used as the electrocatalysts for the hydrogen and oxygen evolution reactions.^{7–9} As one of the least costly technologies for water electrolysis, alkaline liquid electrolyte water electrolysis has been widely deployed for several decades in large-scale hydrogen production.^{7,8} However, the alkaline liquid electrolyte used in these systems, such as aqueous 10 M KOH, can react with carbonate anions formed by adsorption of carbon dioxide from the air to form insoluble species like K₂CO₃. These insoluble carbonates can precipitate in the porous catalyst layers and block the transport of products and reactants, which sharply decreases the electrolyzer performance.²⁰ Alkaline liquid electrolyte water electrolyzers are also

difficult to shut down/start up and their output cannot be ramped quickly because the pressure on the anode and cathode sides of the cell must be equalized at all times to prevent gas crossover through the porous cell separator.

PEM water electrolysis systems offer several advantages over traditional alkaline liquid electrolyte water electrolysis including higher energy efficiency, greater hydrogen production rate, and more compact design.^{11,12,19} These advantages are derived from the solid-state membrane electrolyte compared to a device with free liquid electrolyte and a porous separator. During the past decade, much attention has been paid to the research and development of PEM water electrolysis.^{10–19} However, one of major drawbacks of PEM water electrolysis is the acidic environment, which limits the catalysts to noble metals.¹⁹ In addition, cationic impurities supplied in the feedwater or released from the cell components can bind to the proton conducting site of the PEM/ionomer such as Nafion and reduce its conductivity.¹⁹ Perfluorinated Nafion-based membranes are expensive and have limited chemical diversity for further optimizing their properties. The distinct disadvantage of PEM water electrolysis is its high capital cost of the cell stack compared to alkaline liquid electrolyte water electrolysis. To lower the cost of membrane-based electrolyzers, new materials are needed that enable less expensive electrolyzer systems while maintaining the advantages of the PEM architecture. Critical to this pursuit are new materials that enable membrane-based devices that have high internal pH. Such alkaline membrane technology has been demonstrated for fuel cell operation,^{21–25} but not for water electrolysis.

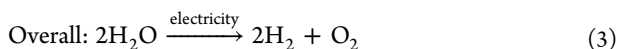
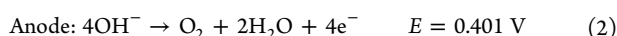
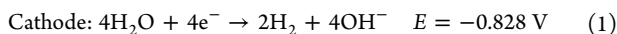
In this work, we report a durable, high performance alkaline membrane water electrolyzer. In this membrane-based architecture, we show key innovations in catalyst layer (CL) design and hydroxide conducting CL ionomer that enable high current densities at low cell potentials. Like alkaline liquid electrolyte water electrolysis, anion exchange membrane (AEM) water electrolysis can potentially employ non-precious metals as the catalysts and cell support structures to make this technology much less expensive than PEM-based systems. Moreover, the quaternary ammonium-based membrane eliminates carbonate precipitation due to the absence of metal cations. Combining the advantages of PEM-based water electrolysis with those of liquid alkaline electrolyte water

Received: March 12, 2012

Published: May 15, 2012

electrolysis makes AEM-based water electrolysis technology promising for applications from hydrogen production to energy storage.

The key element for enabling a high performance alkaline membrane water electrolysis cell is the membrane-electrode assembly (MEA), which consists of anode gas diffusion layer (GDL), anode CL, AEM, cathode CL, and cathode GDL (Figure S1). In a water electrolysis cell, water is consumed at the cathode and reduced to produce hydrogen gas and hydroxide ions (OH^-) (eq 1). The OH^- ions are then transported through the AEM, to the anode. At the anode, OH^- ions are oxidized to produce oxygen gas, water, and electrons (eq 2).



The thermodynamic cell voltage for the overall cell reaction (eq 3) is 1.23 V at 25 °C. For effective production of hydrogen, the applied voltage is required to be >1.23 V to overcome the overpotential of the electrochemical reaction processes and ohmic drop in the cell and achieve a reasonable hydrogen production rate.

Initially, the MEA for the AEM water electrolysis cell was fabricated using the catalyst-coated membrane (CCM) method (see Supporting Information (SI)). Figure 1a shows the polarization curve of an AEM water electrolysis cell based on a MEA with iridium oxide (IrO_2) anode, platinum (Pt) black cathode, AS-4 ionomer (Tokuyama Corp., Japan), and A201 membrane (Tokuyama Corp.) at 50 °C. For the MEA with AS-

4 ionomer-based electrodes, a current density of 399 mA/cm^2 at 1.80 V was obtained, and the high-frequency resistance (HFR) was 0.23 $\Omega \text{ cm}^2$ at 2.0 V. The performance of the AEM water electrolyzer in this work was compared with that of previous reports on PEM and liquid alkaline electrolyte water electrolysis, as shown in Table S1. The performance of the AEM water electrolysis cell reported here was lower than that of PEM water electrolysis by 40–70%. The reasons for the lower performance of AEM based water electrolysis include (1) higher membrane resistance; in this work, HFR $\approx 0.23 \Omega \text{ cm}^2$ at 50 °C, 2 or 3 times higher than that of Nafion-based PEM water electrolysis MEA; (2) lower OH^- conductivity of anion-exchange ionomer used in the CL in this work than the proton conductivity of Nafion ionomer used in PEM electrolysis cell; and (3) possible lower catalyst utilization in the catalyst layer for the AEM water electrolysis cell. Lim²⁵ reported that the electrochemical active area (ECA) of a CCM MEA with 40 wt % Pt/C and AS-4 ionomer used for AEM fuel cell was only 8–12 m^2/g Pt, which was much lower than that for PEM fuel cells, in which the ECA can be $\sim 70 \text{ m}^2/\text{g}$.²⁶ Lim attributed lower catalyst utilization used in AEM fuel cell to the structural differences in Nafion and AS-4 ionomer, and the interaction between Nafion or AS-4 ionomer with the catalysts.²⁵ Similarly, the ECA and the catalysts utilization of the electrode catalysts layer in this work may be much lower than that in PEM-based water electrolysis.

From Table S1, one can find that the performance of the AEM-based water electrolysis cell in this work is comparable with that of alkaline liquid electrolyte water electrolysis cell using non-precious metal catalysts. It is noted that the current performance of AEM-based water electrolysis has been achieved without any optimization. The performance of the AEM-based water electrolyzer can be further improved by optimizing the ionomer content and the structure of the electrode CL, improving the electrodes and MEA fabrication method, and breakthroughs in the development of AEMs and ionomers with high OH^- conductivity.

A critical concern for alkaline membrane technology is durability. It has been well-documented that most AEMs suffer from poor chemical stability.^{27,28} Chemical degradation of AEMs is reported to be mainly due to nucleophilic attack on the cationic fixed charged sites by OH^- .²⁹ This kind of degradation leads to a loss in the number of anion-exchange groups and thus a decrease in OH^- conductivity.²⁹ Since the ionomer used in the catalyst layer is in intimate contact with the catalysts (Figure S1), the chemical or electrochemical degradation of the ionomer may be more severe than that of the membrane. Because of the instability of the membrane and ionomer, most alkaline membrane fuel cells reported in the literature showed lifetimes of <1000 h.^{24,25}

The durability of an MEA with AS-4 ionomer was evaluated under an electrolysis current of 200 mA/cm^2 at 50 °C, and the cell voltage and HFR as a function of test time are shown in Figure 1b. The lifetime for the MEA with AS-4 ionomer was ~ 27 h. To identify the source of degradation, 1 M KOH aqueous solution was supplied to the anode chamber for the degraded MEA and the performance change was measured. Figure 2a shows the change of cell voltage and HFR as a function of test time after 1 M KOH solution was supplied into the anode. The cell voltage under 200 mA/cm^2 decreased sharply from ~ 2.55 to ~ 1.58 V, which was slightly lower than before durability testing (Figure 1). After supply of 1 M KOH solution into the anode, HFR was significantly reduced from

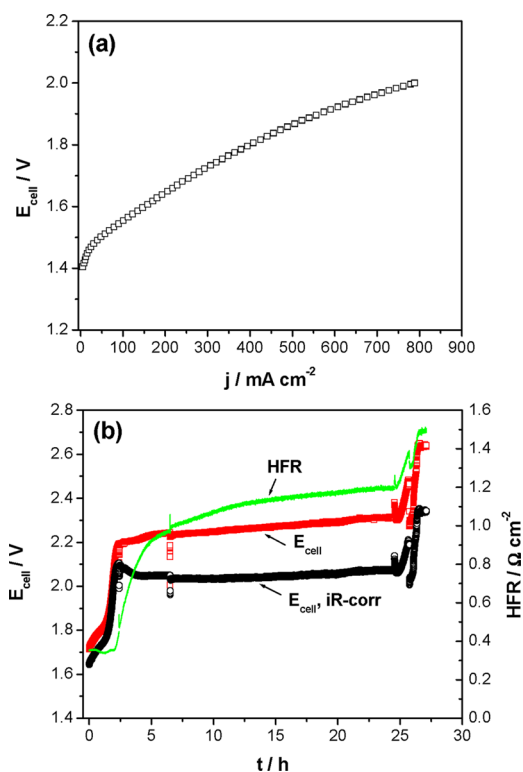


Figure 1. (a) Initial polarization curve and (b) cell voltage and HFR as a function of test time for MEA fabricated with CCM method. Operation conditions: $T = 50$ °C and water cathode-feed mode.

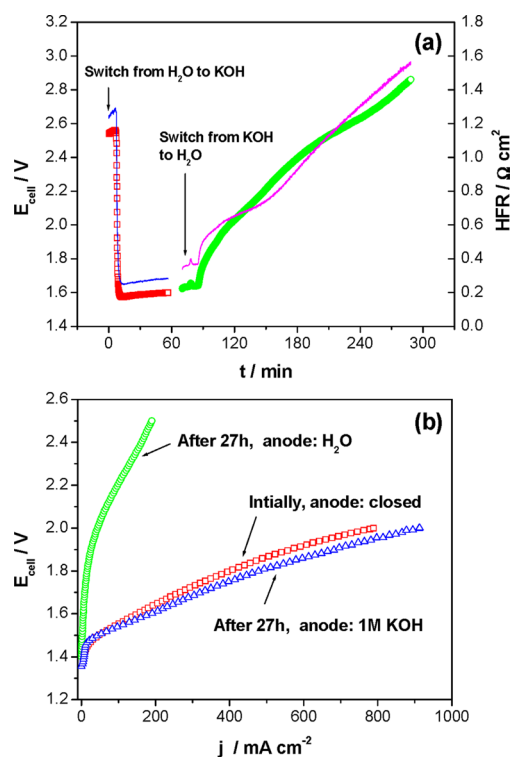


Figure 2. For the degraded MEA with AS-4 ionomer fabricated with CCM method, (a) the change of cell voltage (line plus symbol) and HFR (line) as a function of test time when switching the supply from water to 1 M KOH aqueous solution into the anode chamber, then switching back to water after the test of polarization curve; (b) comparison of the polarization curve after 27 h durability test when supplying water and 1 M KOH into the anode with initial polarization curve before durability test ($T = 50\text{ }^{\circ}\text{C}$; cathode: water, 3 mL/min; anode: water/1 M KOH, 1 mL/min).

1.25 to $0.27\ \Omega\ \text{cm}^2$, which was close to the initial value ($0.23\ \Omega\ \text{cm}^2$) before durability testing. These results indicate that the MEA performance can be recovered to the initial level with 1 M KOH solution supplied into the anode. Figure 2b shows that the MEA performance declined significantly after 27 h durability testing; however, when 1 M KOH aqueous solution was supplied to the anode, the MEA performance recovered. The current density was $480\ \text{mA}/\text{cm}^2$ at 1.80 V, slightly better than the initial level ($399\ \text{mA}/\text{cm}^2$ at 1.80 V in Figure 1a) with fresh AS-4 ionomer. This result was consistent with the galvanostatic test results. When 1 M KOH aqueous solution was supplied to the anode, after the measurement of polarization curve, the galvanostatic test under an electrolysis current density of $200\ \text{mA}/\text{cm}^2$ was resumed. During the resumed galvanostatic test, the supply of 1 M KOH to the anode chamber was switched back to the supply of water at the same flow rate (i.e., 1 mL/min) and the galvanostatic test continued for several hours. The cell voltage and HFR as a function of test time are shown in Figure 2a. As the KOH was gradually flushed from the cell by the inlet water, the cell voltage increased gradually from ~ 1.62 to ~ 2.86 V after ~ 5 h and the HFR also increased gradually from 0.34 to $1.57\ \Omega\ \text{cm}^2$, which was similar to the cell performance after degradation testing and before KOH introduction. From these observations, we conclude that the degradation of MEA in AEM electrolysis cell was mainly due to the degradation of the ionomer and/or membrane-electrode interface.

The durability of the MEA during water electrolysis was significantly improved by adopting a chemically robust ionomer based on a poly(sulfone) backbone³⁰ (see Figure 3 and SI) and

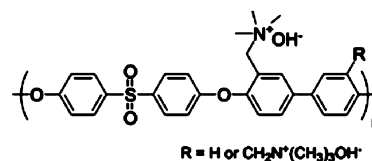


Figure 3. Chemical structure of aminated Radel poly(sulfone).

optimizing the water-feed configuration to the cell. Accelerated degradation studies under high temperature conditions were performed to compare the stability of AS-4 ionomer with the aminated Radel (A-Radel) ionomer. Thermal aging tests (Figures S2 and S3) demonstrated greater stability for A-Radel compared to AS-4, which was correlated to its better long-term performance during electrolyzer operation.

Two types of MEAs were fabricated with catalyst coated substrate (CCS) method (see SI): one with A-Radel ionomer and another of similar construction with AS-4 ionomer. The effect of water feed to the anode or water feed to the cathode on initial performance (Figure S4) and durability of MEA (Figure 4) was explored.

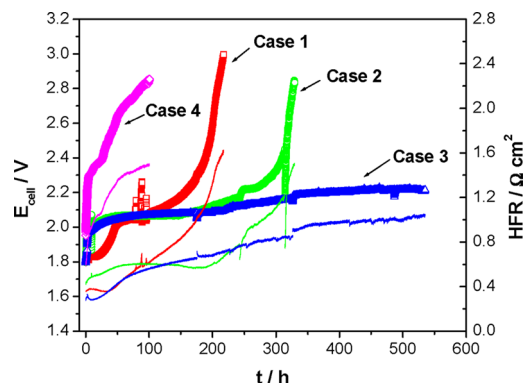


Figure 4. Cell voltage (symbol curve) and HFR (line curve) as a function of test time at $50\text{ }^{\circ}\text{C}$ for four MEAs fabricated with CCS method: case 1, MEA w/A-Radel ionomer, water cathode-feed mode; case 2, MEA w/A-Radel ionomer, water anode-feed mode; case 3, MEA w/A-Radel ionomer, run MEA in water cathode-feed mode for initial 2 h, then switch to water anode-feed mode; case 4, MEA w/AS-4 ionomer, water anode-feed mode.

Durability testing was conducted under an electrolysis current of $200\ \text{mA}/\text{cm}^2$ at $50\text{ }^{\circ}\text{C}$ for four different MEAs (Figure 4). For the case of the MEA with AS-4 ionomer in the water anode-feed mode (case 4), the cell voltage increased significantly with test time, indicating rapid degradation of the MEA, and the HFR showed a strong increase. The HFR includes the contributions from membrane resistance, and contact resistance between electrode catalysts layer and the membrane and/or between the electrode catalysts layer and GDL. The change of HFR as a function of test time is a good indicator for possible combined effects of degradation of the membrane and the delamination between cell components. For the case of MEA with A-Radel ionomer in the water anode-feed mode (case 2), the cell voltage also increased quickly with test time during initial several tens of hours; after that, the cell voltage increased slightly at a relatively low degradation rate

until ~300 h. Similarly, the HFR was nearly constant for ~200 h of durability testing and then increased gradually with the test time. Currently, we cannot identify whether the increase in HFR comes from degradation of ionomer/membrane, or delamination of CLs from the membrane, or both. To identify the sources of cell performance decline, we need to measure the change of hydroxide conductivity in the CL using in situ electrochemical methods^{31,32} and conduct post-mortem analysis of the degraded MEAs. The lifetime (which is defined as the durability test time until the cell voltage reaches a terminal voltage of 2.50 V) for the MEA with A-Radel ionomer was ~317 h, much longer than that for the MEA with AS-4 ionomer (only ~40 h). This result indicated that the A-Radel ionomer was much more durable than the AS-4 ionomer under these test conditions. For the MEAs with A-Radel ionomer (cases 1–3), we also investigated the effect of water-feed mode on the durability of MEA. We found that anode-feed extends the lifetime of MEA. For example, for the MEA with A-Radel ionomer, lifetime in the case of anode-feed mode (case 2) was ~317 h, longer than that in the case of cathode-feed mode (case 1) (~196 h). It is noted that we also demonstrated >535 h of durability test for another MEA with A-Radel ionomer when the MEA was operated in the cathode-feed mode for initial 2 h then switched to the anode-feed mode for the remainder of the test (case 3). For case 3, an initial sharp increase in cell voltage during the first ~20 h of testing was followed by a slow increase with the test time during anode feed mode until ~535 h (the test was stopped due to sudden failure of MEA). Similarly, in case 3, the HFR increased gradually with test time at a relatively low rate until ~535 h, which was consistent with the increasing trend in the cell voltage.

In summary, new methods for constructing solid-state alkaline membrane water electrolyzer MEAs and a stable catalyst layer ionomer are reported. We have demonstrated >500 h of operation of an alkaline membrane electrolysis device at 200 mA/cm² below a cell potential of 2.25 V. The performance of the alkaline membrane device in this work is 30–60% that of an optimized PEM electrolyzer due to ionic conduction losses being greater in AEMs as compared to PEMs. Significant enhancements in durability were achieved by optimizing the catalyst ionomer composition and MEA processing conditions.

Future improvements of alkaline membrane electrolyzers will hinge on creating highly durable ionomers and membranes, incorporating non-precious metal catalysts into the anode and cathode structures, and optimizing MEA configuration and operating conditions. These changes will accelerate the deployment of these types of devices for on-site delivery of hydrogen and new clean energy storage systems.

■ ASSOCIATED CONTENT

● Supporting Information

Experimental procedures, additional figures, data and references. This material is available free of charge via the Internet at <http://pubs.acs.org>.

■ AUTHOR INFORMATION

Corresponding Author

cwx31@psu.edu; hickner@matse.psu.edu

Notes

The authors declare no competing financial interest.

■ ACKNOWLEDGMENTS

This work was funded in part by the Advanced Research Projects Agency – Energy (ARPA-E), U.S. Department of Energy, under Award No. DE-AR0000121. We also thank Tokuyama Corp. for providing A201 membrane and AS-4 ionomer solution.

■ REFERENCES

- (1) Turner, J. A. *Science* **2004**, *305*, 972.
- (2) Cortright, R. D.; Davda, R. R.; Dumesic, J. A. *Nature* **2002**, *418*, 964.
- (3) Zou, Z.; Ye, J.; Sayama, K.; Arakawa, H. *Nature* **2001**, *414*, 625.
- (4) Guerrini, E.; Trasatti, S. In *Catalysis for Sustainable Energy Production*; Barbaro, P., Bianchini, C., Eds.; Wiley-VCH: Weinheim, 2009; p 235.
- (5) Barbir, F. *Solar Energy* **2005**, *78*, 661.
- (6) Gandía, L. M.; Oroz, R.; Ursúa, A.; Sanchis, P.; Diéguez, P. M. *Energy Fuels* **2007**, *21*, 1699.
- (7) Zeng, K.; Zhang, D. K. *Prog. Energy Combust. Sci.* **2010**, *36*, 307.
- (8) Schiller, G.; Henne, R.; Mohr, P.; Peinecke, V. *Int. J. Hydrogen Energy* **1998**, *23*, 761.
- (9) Wendt, H.; Hofmann, H.; Plzak, V. *Mater. Chem. Phys.* **1989**, *22*, 21.
- (10) Rasten, E.; Hagen, G.; Tunold, R. *Electrochim. Acta* **2003**, *48*, 3945.
- (11) Grigoriev, S. A.; Porembsky, V. I.; Fateev, V. N. *Int. J. Hydrogen Energy* **2006**, *31*, 171.
- (12) Marshall, A. T.; Sunde, S.; Tsympkin, M.; Tunold, R. *Int. J. Hydrogen Energy* **2007**, *32*, 2320.
- (13) Marshall, A.; Børresen, B.; Hagen, G.; Tsympkin, M.; Tunold, R. *Energy* **2007**, *32*, 431.
- (14) Cheng, J. B.; Zhang, H. M.; Chen, G. B.; Zhang, Y. N. *Electrochim. Acta* **2009**, *54*, 6250.
- (15) Song, S. D.; Zhang, H. M.; Ma, X. P.; Shao, Z. G.; Baker, R. T.; Yi, B. L. *Int. J. Hydrogen Energy* **2008**, *33*, 4955.
- (16) Zhang, Y. J.; Wang, C.; Wan, N. F.; Liu, Z. X.; Mao, Z. Q. *Electrochem. Commun.* **2007**, *9*, 667.
- (17) Ma, L. R.; Sui, S.; Zhai, Y. C. *Int. J. Hydrogen Energy* **2009**, *34*, 678.
- (18) Wei, G. Q.; Wang, Y. X.; Huang, C. D.; Gao, Q. J.; Wang, Z. T.; Xu, L. *Int. J. Hydrogen Energy* **2010**, *35*, 3951.
- (19) Ayers, K. E.; Anderson, E. B.; Capuano, C. B.; Carter, B. D.; Dalton, L. T.; Hanlon, G.; Manco, J.; Niedzwiecki, M. *ECS Trans.* **2010**, *33*, 3.
- (20) Naughton, M. S.; Brushett, F. R.; Kenis, P. J. A. *J. Power Sources* **2011**, *196*, 1762.
- (21) Varcoe, J. R.; Slade, R. C. T.; Yee, E. L. H. *Chem. Commun.* **2006**, 1428.
- (22) Yanagi, H.; Fukuta, K. *ECS Trans.* **2008**, *16*, 257.
- (23) Lu, S. F.; Pan, J.; Huang, A.; Zhuang, L.; Lu, J. T. *Proc. Natl. Acad. Sci. U.S.A.* **2008**, *105*, 20611.
- (24) Piana, M.; Boccia, M.; Filpi, A.; Flammia, E.; Miller, H. A.; Orsini, M.; Salusti, F.; Santiccioli, S.; Ciardelli, F.; Pucci, A. *J. Power Sources* **2010**, *195*, 5875.
- (25) Lim, P. C. Ph.D. Dissertation, Pennsylvania State University, 2008.
- (26) Ge, S. H.; Wang, C. Y. *J. Electrochem. Soc.* **2007**, *154*, B998.
- (27) Varcoe, J. R.; Slade, R. C. T. *Fuel Cells* **2005**, *5*, 187.
- (28) Bauer, B.; Strathmann, H.; Effenberger, F. *Desalination* **1990**, *79*, 125.
- (29) Arges, C. G.; Ramani, V.; Pintauro, P. N. *Electrochem. Soc. Interface* **2010**, *19*, 31.
- (30) Hibbs, M. R.; Hickner, M. A.; Alam, T. M.; McIntyre, S. K.; Fujimoto, C. H.; Cornelius, C. J. *Chem. Mater.* **2008**, *20*, 2566.
- (31) Makharia, R.; Mathias, M. F.; Baker, D. R. *J. Electrochem. Soc.* **2005**, *152*, A970.
- (32) Liu, Y.; Murphy, M. W.; Baker, D. R.; Gu, W.; Ji, C.; Jorne, J.; Gasteiger, H. A. *J. Electrochem. Soc.* **2009**, *156*, B970.